THE JOURNAL OF PHYSICAL CHEMISTRY A

Article

pubs.acs.org/JPCA

Structural, Energetic, and UV−Vis Spectral Analysis of UVA Filter 4-*tert*-Butyl-4′-methoxydibenzoylmethane

Luís Pinto da Silva,[†] Paulo J. O. Ferreira,[†] Darío J. R. Duarte,[‡] Margarida S. Miranda,*[,§] and Joaquim C. G. Esteves da Silva[†]

[†]Centro de Investigação em Química, Departamento de Química e Bioquímica, Faculdade de Ciências, Universidade do Porto, Rua do Campo Alegre, s/n, P-4169-007 Porto, Portugal

[‡]Laboratorio de Estructura Molecular y Propiedades, Área de Química Física-Departamento de Química, Facultad de Ciencias Exactas y Naturales y Agrimensura, Universidad Nacional del Nordeste, Avenida Libertad 5460, (3400) Corrientes, Argentina

[§]Centro de Geologia da Universidade do Porto, Faculdade de Ciências, Universidade do Porto, Rua do Campo Alegre, s/n, P-4169-007 Porto, Portugal

Supporting Information

ABSTRACT: The growing awareness of the harmful effects of ultraviolet (UV) solar radiation has increased the production and consumption of sunscreen products, which contain organic and inorganic molecules named UV filters that absorb, reflect, or scatter UV radiation, thus minimizing negative human health effects. 4-*tert*-Butyl-4′-methoxydibenzoylmethane (BMDBM) is one of the few organic UVA filters and the most commonly used. BMDBM exists in sunscreens in the enol form which absorbs strongly in the UVA range. However, under sunlight irradiation tautomerization occurs to the keto form, resulting in the loss of UV protection. In this study we have performed quantum chemical calculations to study the excited-state molecular structure and excitation spectra of the enol and keto tautomers of BMDBM. This knowledge is of the utmost importance as the starting point for studies aiming at the understanding of its activity when applied on human skin and also its fate once released into the aquatic environment. The efficiency of excitation transitions was rationalized based on the concept of molecular orbital superposition. The loss of UV protection was attributed to the enol → keto phototautomerism and subsequent photodegradation. Although this process is not energetically favorable in the singlet bright state, photodegradation is possible because of intersystem crossing to the first two triplet states.

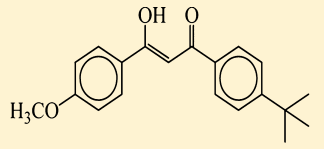

4-*tert*-butyl-4`-methoxydibenzoylmethane

INTRODUCTION

The raising level of awareness regarding the harmful effects of solar radiation has resulted in an increase in the production and consumption of sunscreens. These commercial products contain ultraviolet (UV) filters that absorb, reflect, or scatter UV radiation (290−320 nm for UVB and 320−400 nm for UVA), preventing sunburn, photoaging, and ultimately skin diseases such as skin cancer. Nowadays these compounds are incorporated into not only sunscreens but also a number of personal care products and even in plastics, varnishes, and clothes to enhance their light stability. However, a number of UV filters have shown to present toxic effects; thus, maximum concentrations have been established (up to 10%, w/w) with a compromise between adequate protection and minimal side effects for users.[1]

There are few organic UV filters that provide protection in the UVA region. Of these 4-*tert*-butyl-4′-methoxydibenzoylmethane (trade names avobenzone, Parsol 1789, Eusolex 9020, etc.), here abbreviated as BMDBM, is the most widely used. BMDBM belongs to the dibenzoylmethanes class of UV filters,[2] which in turn belongs to the larger family of the β-diketones. BMDBM and β-diketones in general are known to exist in two tautomeric forms: the enol and keto forms. The preference for the enol form is due to the stabilization gained by the formation of an intramolecular hydrogen bond (IMHB).[3−7] In the case of BMDBM, because the enol tautomer is asymmetric, it has two isomeric cis-enol tautomers, as shown in Figure 1, whereas the keto tautomer occurs in only one form.

In sunscreen formulations, BMDBM exists predominantly in the enol form, which absorbs in the UVA wavelength range. The enol form displays high molar absorption coefficients with a maximum at wavelengths ranging from 340 to 365 nm depending on the solvent used.[8−11] In solution an equilibrium mixture of the enol and keto tautomers is present.

The relative amount of the two tautomers depends on the solvent, but the equilibrium always lies in the direction of the enol tautomer. The keto tautomer absorbs in the UVC range from 260 to 280 nm. Under the presence of sunlight (or artificial irradiation), the enol tautomer transforms into the keto tautomer, accounting for the large loss in absorption in the UVA range and thus reducing the effectiveness of the sunscreen. Moreover, the photoproducts may promote allergies on human skin.[12] Huong et al.[9] have found that under irradiation the enol form of BMDBM tautomerizes to the keto

Received: October 21, 2013
Revised: February 3, 2014
Published: February 4, 2014

dx.doi.org/10.1021/jp4123375 | *J. Phys. Chem. A* 2014, 118, 1511−1518

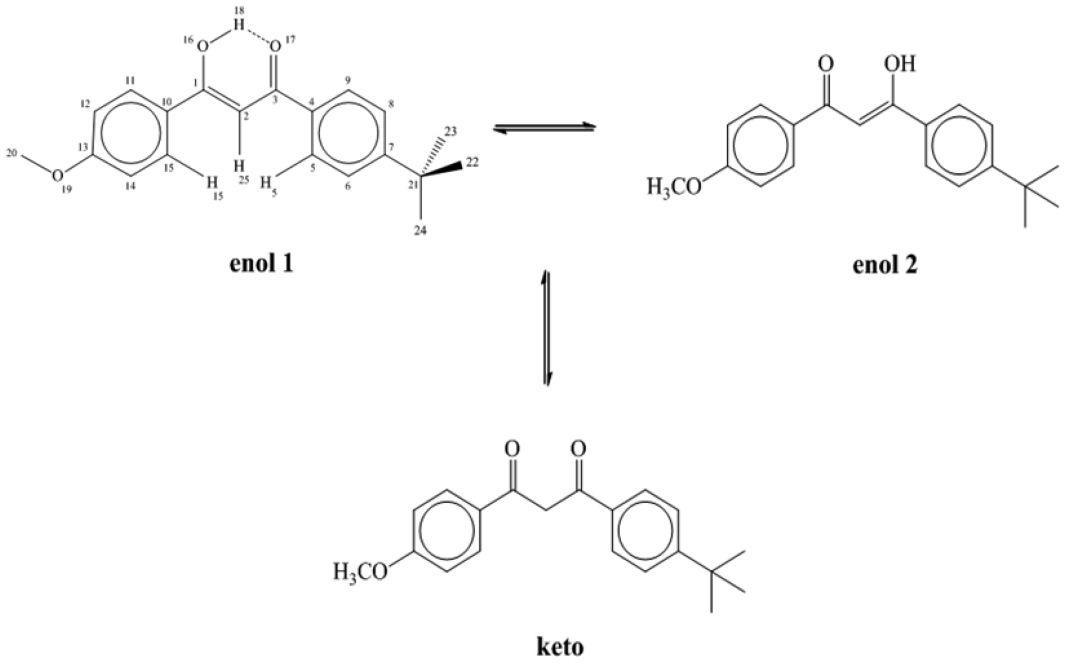

Figure 1. Tautomeric structures of 4-*tert*-butyl-4′-methoxydibenzoylmethane (BMDBM). For enol 2, the same atom numbering was used as for enol 1 but the O−H bond is O_{17}−H_{18} and the intramolecular O···H interaction is O_{16}···H_{18}.

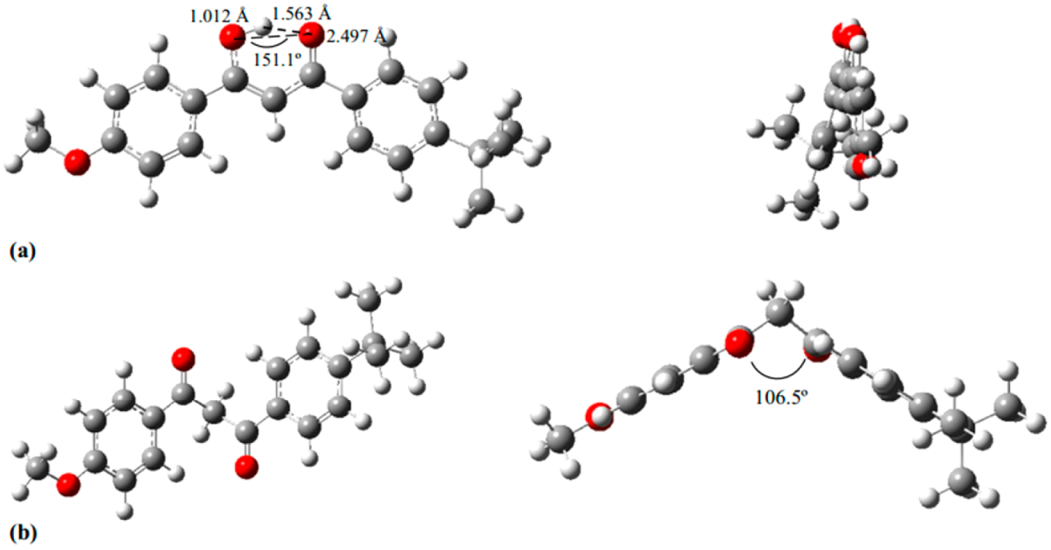

Figure 2. Front and side views of the B3LYP/6-311++G(d,p) optimized molecular structure of the enol (a) and keto (b) tautomers of BMDBM.

form and is also fully photodegraded, resulting in a complete loss of UV protection. This has been shown to occur in diluted and concentrated solutions of various solvents including water and in films of commercial sunscreens. The authors identified various photoproducts: substituted benzoic acids, benzils, dibenzoylmethanes, and dibenzoylethanes. Some of these compounds were also previously proposed by Schwack and Rudolph.[10] These authors argued that the formation of these photoproducts involves primary α bond cleavages of carbonyl groups of the diketo form, followed by hydrogen abstraction and/or oxidation or radical recombination.

Despite the practical importance of UVA filter BMDBM, information about the excited-state structure and energetics of its tautomers is very scarce. This knowledge is of the utmost importance as a starting point for studies aiming at the understanding of its activity once applied on human skin and also its fate when released into the aquatic environment. Recent studies have recognized the accumulation of organic UV filters in the aquatic environment, especially bathing waters. The occurrence of UV filters has been reported in surface water such as lakes, rivers, and seas as well as in wastewater, tap water, and swimming pools.[13,14] UV filters may enter surface waters directly (when released from skin during bathing and swimming) or indirectly via wastewater treatment plants (when released during showering or washed from textiles).[14] BMDBM has already been detected in surface waters, wastewater, and biota.[13]

We have performed density functional theory (DFT) calculations with the B3LYP density functional and the 6-31G(d) and 6-311++G(d,p) basis sets to obtain the gas-phase molecular structure and energetic stability of the enol and keto tautomers of BMDBM. We have also used the CAM-B3LYP

dx.doi.org/10.1021/jp4123375 | J. Phys. Chem. A 2014, 118, 1511−1518

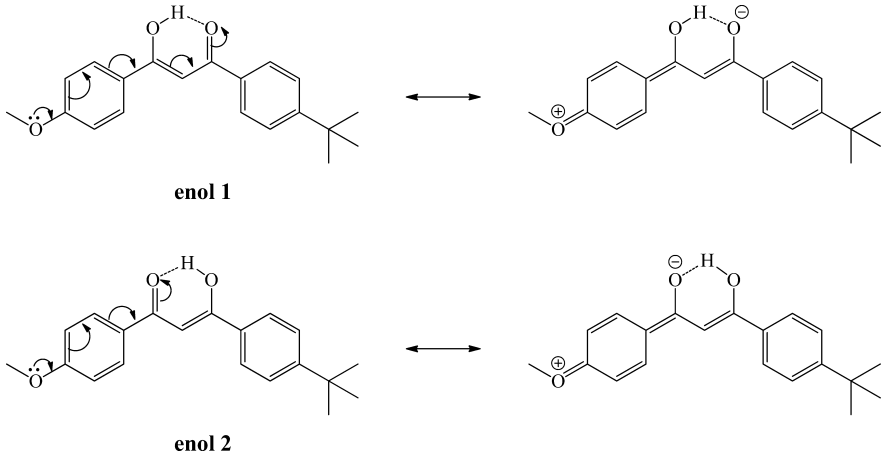

Figure 3. Resonance structures of enol 1 and enol 2 of BMDBM showing the extended π electron delocalization between the methoxy group, benzene ring, and enol moiety.

functional in implicit solvents (water, ethanol, and cyclohexane) with the 6-31+G(d) basis set in order to analyze the excited-state properties of the three tautomers of BMDBM.

COMPUTATIONAL DETAILS

The geometries of all molecules were fully optimized using density functional theory (DFT) with the B3LYP three-parameter hybrid functional proposed by Becke[15−17] and the 6-31G(d) basis set. The obtained optimum structures were reoptimized using the more extended 6-311++G(d,p) basis set to get more reliable molecular structures and energies. The stationary points found at each level of theory were characterized as true minima through construction and diagonalization of the Hessian matrix.

Calculations were also performed in water, ethanol, and cyclohexane by means of the self-consistent reaction field (SCRF) method based on the polarizable continuum model (PCM) of Tomasi and co-workers.[18−20] In this model, the molecule under study, solute, is placed inside a cavity of a convenient shape and the solvent is defined by a continuous medium, which is characterized by its dielectric constant.

The excitation transitions of the keto and enol tautomers of BMDBM were calculated at the time-dependent (TD) CAM-B3LYP/6-31+G(d) level of theory.[21,22] This long-range corrected functional was used as it provides good estimates for both local $n \rightarrow \pi^*$ and $\pi \rightarrow \pi^*$ states, as well for charge transfer and Rydberg excited states.[23] To obtain the excitation spectra of the studied species, six excited states were calculated. The molecular orbitals that contributed for the transitions of interest were obtained with the Gabedit program.[24]

All calculations were performed with the *Gaussian* 09 series of programs (revision A.02).[25]

RESULTS AND DISCUSSION

In Figure 2 we show the most stable conformations found for the three tautomers of BMDBM after conformational search (data not shown).

The benzene ring containing the *tert*-butyl group is slightly outside the plane of the rest of the molecule: dihedral angle $C_2-C_3-C_4-C_5$ is 14.8° in enol 1 and 14.1° in enol 2. The enolic moiety is almost planar in both enols of BMDBM, and the hydrogen atom of the hydroxyl group is pointing toward the oxygen atom of the C═O bond, establishing an intramolecular hydrogen bond (O···H−O). The interaction O−H···O═C may be qualified as a resonance-assisted hydrogen bond (RAHB).[6,7] The RAHB is a model of synergistic interplay between π delocalization and hydrogen bond strengthening proposed by Gilli et al.[6,7] for explaining the abnormally strong intramolecular hydrogen bonds formed in the enol moiety of β-diketones.

IMHB energies (ΔE_{IMHB}) were calculated, and the following values were obtained: 71.1 kJ/mol for enol 1 and 69.8 kJ/mol for enol 2. The benzene ring containing the methoxy group is almost in the same plane of the enol moiety: dihedral angle $C_2-C_1-C_{10}-C_{15}$ is 2.6° in enol 1 and 2.9° in enol 2. The planar arrangement of the methoxy group allows the existence of extended electron delocalization with the enolic moiety through the benzene ring (Figure 3) with the consequent energetic stabilization and ΔE_{IMHB} values.

The most stable conformation of the keto tautomer of BMDBM has a very distorted geometry with a "butterfly" shape (Figure 2b). However, the two substituted dibenzoyl rings are almost planar and form an angle of 106.5°.

The excited-state properties of the keto and enol tautomers of BMDBM, at the Franck−Condon state within the vertical approximation, were calculated at the CAM-B3LYP/6-31+G(d) level of theory in implicit water, ethanol, and cyclohexane. The excitation wavelengths, oscillator strengths, and excitation transitions are presented in Table 1.

The keto tautomer of BMDBM appears to absorb light in the UVC region (100−290 nm), while the two enol tautomers absorb in the UVA region (320−400 nm). The calculated

Table 1. Excitation Wavelengths (λ_{ex}), Oscillator Strengths (f), and the Excited-State Transitions Referent to the Bright State for the Three Tautomers of BMDBM

	BMDBM tautomer	λ_{ex} (nm)	f	transitions
water	keto	280	0.7224	$S_0 \rightarrow S_3$
	enol 1	340	1.3028	$S_0 \rightarrow S_1$
	enol 2	335	1.3534	$S_0 \rightarrow S_1$
ethanol	keto	279	0.7144	$S_0 \rightarrow S_3$
	enol 1	339	1.2955	$S_0 \rightarrow S_1$
	enol 2	334	1.3454	$S_0 \rightarrow S_1$
cyclohexane	keto	270	0.6003	$S_0 \rightarrow S_3$
	enol 1	323	1.1766	$S_0 \rightarrow S_1$
	enol 2	320	1.2164	$S_0 \rightarrow S_1$

dx.doi.org/10.1021/jp4123375 | J. Phys. Chem. A 2014, 118, 1511−1518

excitation wavelengths of all three molecules is in agreement with known experimental values.[8,9] Besides absorbing light in an UV region different than that of the two enol tautomers, the keto tautomer presents a lower excitation efficiency. This is in agreement with the experimental data that indicates that the enol → keto phototautomerism accounts for a loss in the absorption.[8,9] Moreover, while the excitation of the enol tautomers consist of $S_0 \rightarrow S_1$ transitions, the excitation of the keto tautomer consists of a $S_0 \rightarrow S_3$ transition. Thus, our calculations show that both enols have very similar properties at the Franck−Condon state, while the keto tautomer has different properties.

The properties at the Franck−Condon state are also affected by the solvent medium. While there is no great difference between the excitation wavelengths at water and ethanol, the computed excitation is blue-shifted in cyclohexane for both enol and keto species (Table 1). Moreover, we can see that the excited-state transition efficiency has a direct correlation with the polarity of the solvent (Table 1).

There are various tools based on theoretical chemistry that can be used in the analysis of inter- and intramolecular interactions. In this study we have used the quantum theory of atoms in molecules (QTAIM) to characterize intramolecular noncovalent interactions of the three tautomers of BMDBM at the Franck−Condon state.[26] The QTAIM analysis was performed with the Multiwfn code.[27] In Figure 4 we present the three tautomers with the ring critical points (RCP), bond critical points (BCP), and the paths that connect the BCP, as calculated by Multiwfn.

In QTAIM analysis an interaction can be studied by characterizing the associated BCP. There are several parameters that can be derived by QTAIM to define the bonding nature in the BCP region: the value of electron density distribution $\rho(r_b)$, Laplacian $\nabla^2\rho(r_b)$, ellipticity ε, total electron energy density $H(r_b)$, and the ratio $-(G(r_b)/V(r_b))$. $G(r_b)$ refers to the Lagrangian kinetic energy, while $V(r_b)$ is a measure of the potential energy density. The values of these parameters are presented for three tautomers in water in Table 2. The results in ethanol and in cyclohexane are presented in the Supporting Information.

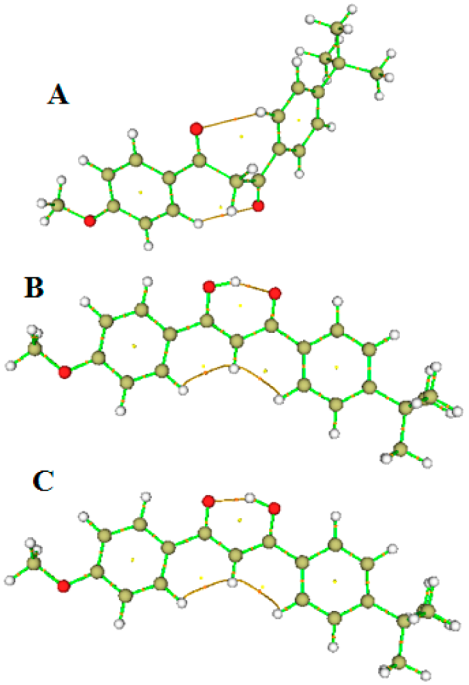

Figure 4. Representation of keto (A), enol 1 (B), and enol 2 (C), and their respective BCP, bond paths, and RCP.

Figure 4A indicates that keto has two O···H−C hydrogen bonds. The positive value of $\nabla^2\rho(r_b)$ and the low value of $\rho(r_b)$ indicate that this is a closed shell interaction.[28,29] The ellipticity provides a measure of π or σ character of a bond and also its structural stability.[30] As the values of ε are below 0.1, these two hydrogen bonds have σ bond character. The $-(G(r_b)/V(r_b))$ ratio is an important measure for the nature of the bonds.[31] For values above 1, the bond is noncovalent. Between 0.5 and 1, this ratio indicates that the bond is partially covalent.[31] As expected, the $-(G(r_b)/V(r_b))$ ratio indicates that these hydrogen bonds are noncovalent. Rozas and co-workers proposed a classification of hydrogen bonds based on the values of $\nabla^2\rho(r_b)$ and $H(r_b)$.[32] Positive $\nabla^2\rho(r_b)$ and $H(r_b)$ values indicate weak to medium strength in hydrogen bonds. For strong hydrogen bonds, $\nabla^2\rho(r_b)$ is positive and $H(r_b)$ negative. When both $\nabla^2\rho(r_b)$ and $H(r_b)$ values are negative, the interaction is a very strong hydrogen bond. According to this classification, both O···H−C hydrogen bonds are weak to medium in strength.

Figure 4B,C indicates that excited-state enol 1/2 present similar intramolecular interaction. Besides the intramolecular hydrogen bond (O···H−O), there is also an interaction between hydrogen atoms 5, 15, and 25. The positive values of $\nabla^2\rho(r_b)$ and the low values of $\rho(r_b)$ indicate that all these interactions are closed shell interactions. The obtained ε values indicate that the interactions between hydrogen atoms (5, 15, and 25) have structural instability; that is, the bond can easily be ruptured, while the obtained ε values to the O···H−O hydrogen bonds indicate a σ bonding character. In contrast to the O···H−C hydrogen bonds in excited-state keto, the O···H−O hydrogen bonds in excited-state enol 1/2 have partially covalent character (by analysis of the $-(G(r_b)/V(r_b))$ ratio). This finding indicates that the O···H−O hydrogen bonds should be strong interactions. The closed shell interactions between hydrogen atoms (5, 15, and 25) are noncovalent. The values of $H(r_b)$ (negative), along with the positive values of $\nabla^2\rho(r_b)$, confirms that the excited-state O···H−O hydrogen bonds are strong. None of the conclusions obtained with the QTAIM analysis are affected by the nature of the solvent (water, ethanol, or cyclohexane).

We have further analyzed the excitation transitions of the three BMDBM tautomers by studying the excitation contributions that compose the already referred transitions (Table 3). We present only the values obtained in implicit water, as excitation contributions are very similar in all solvents.

The $S_0 \rightarrow S_3$ transition of the keto tautomer consists of a highest occupied molecular orbital (HOMO) → lowest unoccupied molecular orbital (LUMO) (68.2%) and a HOMO → LUMO(+1) (25.6%) excitation. The $S_0 \rightarrow S_1$ transition of enol 1 consists of only a HOMO → LUMO (90.0%) excitation. In the case of enol 2, the HOMO → LUMO (89.1%) excitation is also dominant, but there is also a small contribution from HOMO(−1) → LUMO (4.2%) orbital excitation.

In Figure 5 we present the HOMO, LUMO, and LUMO(+1) orbitals of the keto tautomer in water.

It can be seen that the HOMO orbital is localized in the methoxybenzoyl moiety, while the LUMO and LUMO(+1)

dx.doi.org/10.1021/jp4123375 | J. Phys. Chem. A 2014, 118, 1511−1518

Table 2. $\nabla^2\rho(r_b)$, $\rho(r_b)$, ε, $H(r_b)$, and $-(G(r_b)/V(r_b))$ Values for the Relevant BCP, for the Three BMDBM in Water[a]

	interactions	$\nabla^2\rho(r_b)$	$\rho(r_b)$	ε	$H(r_b)$	$-(G(r_b)/V(r_b))$
keto	O···H−C	0.04	0.01	0.04	0.001	1.1
	O···H−C	0.04	0.01	0.06	0.001	1.1
enol 1	O···H−O	0.19	0.07	0.01	−0.007	0.9
	H···H···H	0.04	0.01	1.23	0.003	1.5
	H···H···H	0.05	0.01	0.83	0.003	1.5
enol 2	O···H−O	0.19	0.07	0.01	−0.006	0.9
	H···H···C	0.05	0.01	0.75	0.003	1.4
	H···H···C	0.05	0.01	1.55	0.003	1.5

[a]All values are in atomic units except for ε and $-(G(r_b)/V(r_b))$ that are dimensionless.

Table 3. Contributions (in Percentage) from the Orbital Excitations That Compose the Excited-State Transitions for the Three Tautomers of BMDBM in Implicit Water

excitation transitions	keto	enol 1	enol 2
HOMO(−1) → LUMO	–	–	4.2
HOMO → LUMO	68.2	90.0	89.1
HOMO → LUMO(+1)	25.6	–	–

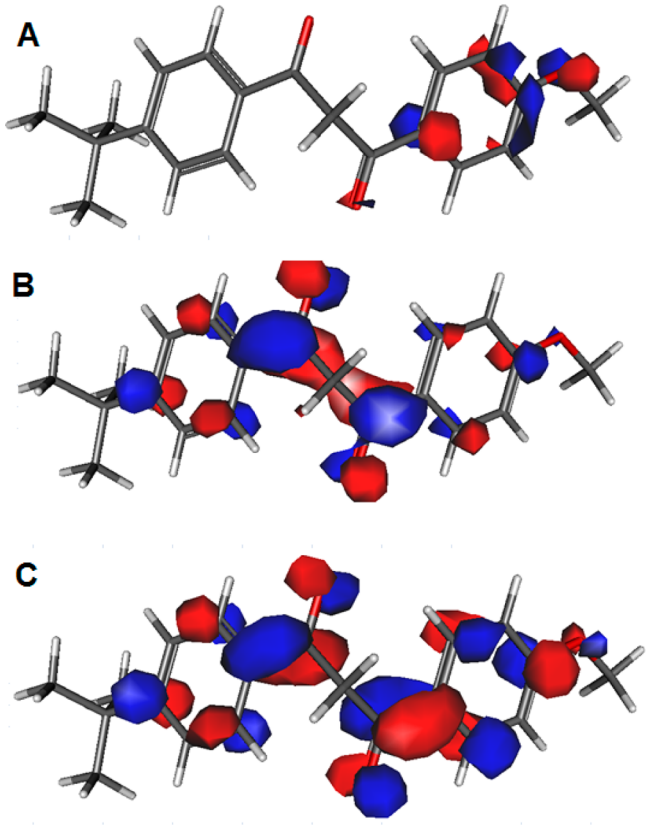

Figure 5. HOMO (A), LUMO (B), and LUMO(+1) orbitals of the keto tautomer of BMDBM in water.

orbitals are delocalized along the dibenzoyl scaffold. A somewhat similar scenario is seen for enol 1, also in water (Figure 6).

The HOMO orbital is localized mainly on the methoxybenzoyl moiety, but it can also be seen on the other benzoyl ring. In the case of the LUMO, the orbital is more delocalized between the dibenzoyl scaffold. For the case of enol 2 in water, both the HOMO and LUMO orbitals are delocalized between the dibenzoyl scaffold (Figure 7). It should be noted that for

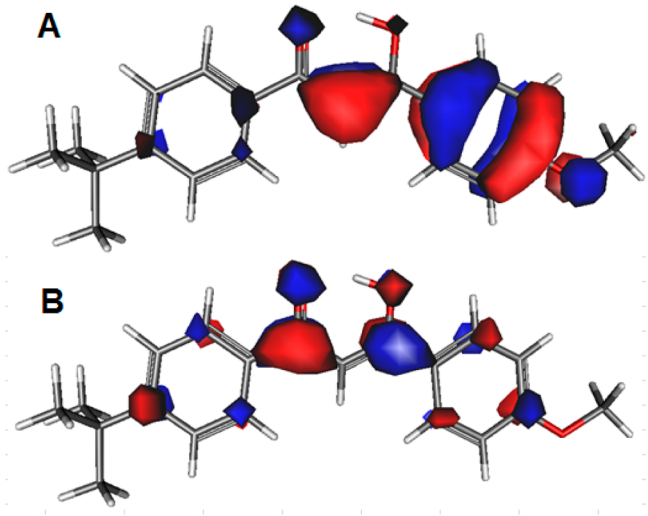

Figure 6. HOMO (A) and LUMO (B) orbitals of BMDBM enol 1 tautomer in water.

the excited-state transitions, the *tert*-butyl and methoxy moieties appear to have little to no effect in the process.

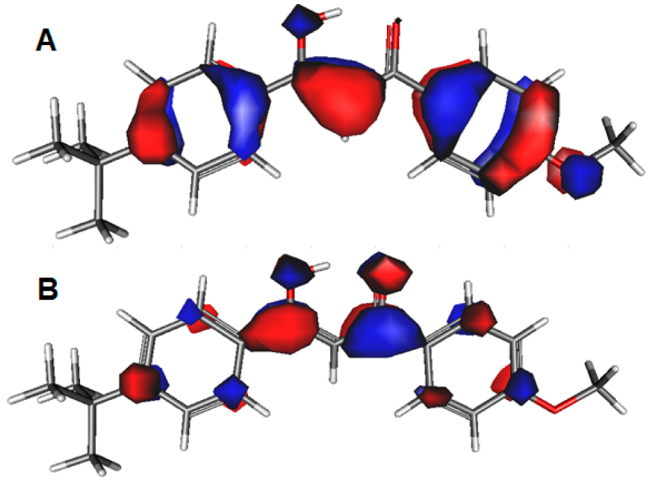

Figure 7. HOMO (A) and LUMO (B) orbitals of BMDBM enol 2 tautomer in water.

The position of the orbitals in the three molecules may help to explain their excitation efficiencies (Table 1). In the case of enol 2, the one with higher excitation efficiency, the contributing orbitals are both delocalized between the dibenzoyl scaffold. Therefore, there is apparently a superposition of orbitals, which is expected to facilitate the excitation

dx.doi.org/10.1021/jp4123375 | J. Phys. Chem. A 2014, 118, 1511−1518

and consequently the $S_0 \rightarrow S_1$ transition. The tautomer with the second higher excitation efficiency is enol 1. Also in this case, the concept of orbital superposition appears to be of importance. The LUMO orbital is delocalized between the dibenzoyl scaffold, while the majority of the HOMO orbital resides in the methoxybenzoyl moiety. Nevertheless, there is a small presence of HOMO orbital in the other benzoyl group, which increases the superposition of HOMO/LUMO and thereby the efficiency of transition. Finally, in the tautomer with lower excitation efficiency (keto), both LUMO and LUMO-(+1) are delocalized between the dibenzoyl system. In contrast, the HOMO resides only on the methoxybenzoyl moiety, which decreases the superposition and the efficiency of excited-state transition. Thus, a higher delocalization of HOMO between the dibenzoyl scaffold should increase the excitation efficiency, as both LUMO and LUMO(+1) present such delocalization in all three BMDBM species.

Similar conclusions can be derived from the analysis of the molecular orbitals of BMDBM tautomers in ethanol and cyclohexane (Figures S1−S6 of Supporting Information). The concept of orbital superposition still appears to be useful in the explanation of the efficiency of excited-state transition. In general, orbital superposition in ethanol and cyclohexane is lower than that in water (for the three BMDBM species), which is in agreement with the higher f value found for the latter solvent (Table 1).

By analysis of excitation-induced fragmentation products of BMDBM, we see that there must be a bond breaking between carbon atoms C_{1-3} (see Figure 1 for atom numbering).[9] In Table 4 we present the ESP atomic charges of these atoms for the three BMDBM tautomers, both in the ground and excited states.

Table 4. ESP Atomic Charges of the C_{1-3} Atoms in Both the Ground (S_0) and Excited States (S_1 or S_3) for the Three Tautomers of BMDBM[a]

BMDBM tautomer	state	C_1	C_2	C_3
keto	S_0	0.625	−0.225	0.583
	S_3	0.388	−0.166	0.501
enol 1	S_0	0.711	−0.919	0.778
	S_1	0.577	−0.655	0.614
enol 2	S_0	0.938	−0.913	0.597
	S_1	0.756	−0.635	0.483

[a]See Figure 1 for atom numbering scheme.

By analysis of Table 4, one cannot attribute solely the photodegradation process to changes in the interaction of C_{1-3} atoms upon photoexcitation. The central atom (C_2) is negative in all tautomers and in both states, while C_1 and C_3 present positive charge. This indicates that C_1-C_2 and C_2-C_3 bonds are electrostatically favorable. However, the positive charge of $C_{1,3}$ and the negative charge of C_2 decrease upon photoexcitation, indicating that the C_1-C_2 and C_2-C_3 bonds are stronger in the ground state. The association with enol → keto phototautomerism with photodegradation is supported by the evidence that the charge difference between $C_{1/3}$ and C_2 in the case of excited-state keto is lower than that in the case of the enol species.

We have further studied the process of photodegradation by performing a relaxed C_1-C_2 bond length scan, a bond assumed to be broken during the process of keto species fragmentation.[9,10] Our calculations support this assumption. The calculations of the ESP charges of C_{1-3} (Table 4) showed that both C_1-C_2 and C_2-C_3 bonds should be stabilized by attractive electrostatic interactions. However, the charge difference in the C_2-C_3 bond (0.667) is higher than that in the C_1-C_2 bond (0.554). This indicates that the C_2-C_3 bond should be more stabilized by electrostatic and polarizability factors than the C_1-C_2 bond, making this latter bond the most probable one to break upon phototautomerism. Moreover, QTAIM analysis of C_1-C_2 and C_2-C_3 bonds at the bright singlet state of keto shows that the former bond is weaker than the latter. The value of $H(r_b)$ for the C_1-C_2 BCP ($H(r_b)$ = −0.191, in atomic units) is less negative than the same parameter for the C_2-C_3 BCP ($H(r_b)$ = −0.198, in atomic units), thus supporting the assumption made by other researchers.[9,10]

The photodegradation potential energy surfaces (PES) were obtained by calculating the Franck−Condon curves by adding the TD-CAM-B3LYP/6-31+G(d) vertical excitation energies to the CAM-B3LYP/6-31+G(d)//B3LYP/6-31G(d) ground-state energies. The relaxed scan was performed in the gas phase, while the energies were obtained in implicit water. Such a strategy has been successfully implemented to evaluate excited-state reactions.[33−35] The results are presented in Figure 8.

By analysis of Figure 8, it can be seen that the photodegradation process is not very favorable in the PES of the singlet bright state. The energy increases steadily during the increase of the C_1-C_2 bond from 1.54 to 2.74 Å. This indicates that the photodegradation process does not involve only enol

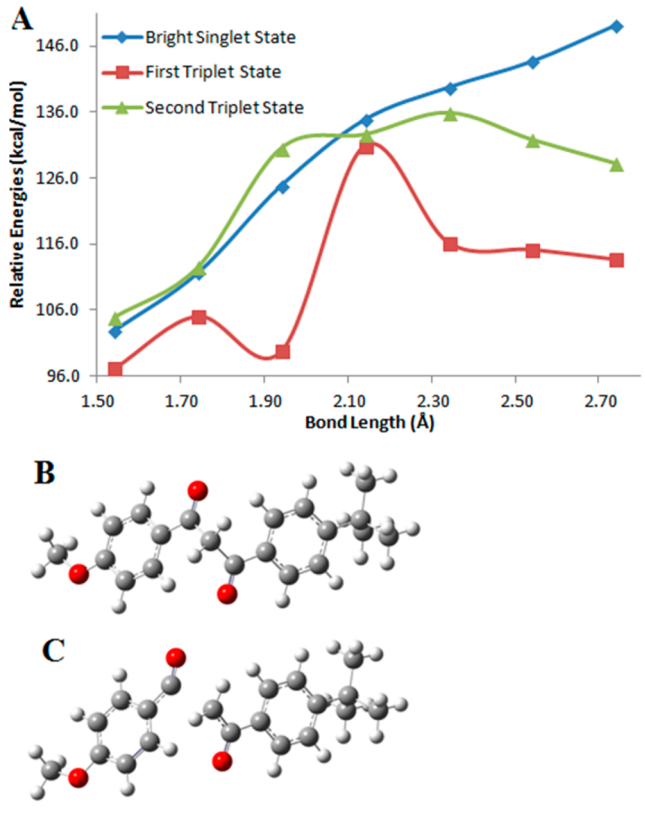

Figure 8. Relative energies (in kilocalories per mole) of the bright singlet state and the first two triplet excited states (A). The energies are relative to the energy of the singlet ground state of keto species at C_1-C_2 bond length of 1.54 Å. Representation of keto with C_1-C_2 bond length of 1.54 (B) and 2.74 (C) Å.

dx.doi.org/10.1021/jp4123375 | J. Phys. Chem. A 2014, 118, 1511−1518

→ keto phototautomerism. Nevertheless, Figure 8 sheds some light to this topic. At C_1-C_2 bond length of 1.54 and 1.74 Å, the singlet excited state and the second triplet energy differ by only 2.0 and 0.8 kcal/mol. At bond length of 1.94 Å, both states now differ by 5.6 kcal/mol. However, while in the C_1-C_2 bond length range of 1.54−1.94 Å, the energy of the second triplet state is higher than that of the singlet state; from bond length of 2.14 Å onward the second triplet state is the one lower in energy. These findings indicate that the possibility exists for intersystem crossing between these two states. Moreover, at C_1-C_2 bond length of 2.14 Å there is a possibility for second → first triplet excited-state transition, given the low energetic difference (1.7 kcal/mol). It should be noted that the energy decreases (in a general way) from C_1-C_2 bond length of 2.14 Å onward. Thus, our results indicate that the photodegradation occurs as a result of intersystem crossing from the keto species bright singlet excited state to triplet states, in which the PES of the C_1-C_2 bond breaking is more energetically favorable.

CONCLUSIONS

The present computational study allowed us to obtain new and important structural and energetic parameters that characterize the excited state of UVA filter 4-tert-butyl-4′-methoxydibenzoylmethane (BMDBM).

The most stable conformations of enol and keto tautomers BMDBM were computed with the B3LYP/6-311++G(d,p) level of theory. The enol tautomers were found to be more stable than the keto because of the existence of an intramolecular resonance-assisted hydrogen bond (RAHB). Noncovalent intramolecular interactions were analyzed by QTAIM at the Franck−Condon state for all tautomers. Our calculations correctly describe the excitation wavelengths of the three tautomers of BMDBM. The efficiency of ground → excited states transition was rationalized based on the concept of molecular orbital superposition. The loss of UV protection was attributed to the enol → keto phototautomerism and subsequent C_1-C_2 bond breaking. Although this process is not energetically favorable in the singlet bright state, intersystem crossing to the first two triplet states results in photodegradation.

ASSOCIATED CONTENT

Supporting Information

Singlet ground-state structure of the three BMDBM tautomers (Tables S1−S3) and molecular orbitals of BMDBM tautomers in ethanol and cyclohexane (Figures S1−S6). This material is available free of charge via the Internet at http://pubs.acs.org.

AUTHOR INFORMATION

Corresponding Author

*E-mail: msmirand@fc.up.pt. Tel.: 00 351 22 0402 568.

Notes

The authors declare no competing financial interest.

ACKNOWLEDGMENTS

A Ph.D. Grant to L.P.d.S. (SFRH/BD/76612/2011), attributed to FCT, is also acknowledged. M.S.M. thanks Fundação para a Ciência e a Tecnologia, FCT, Lisbon, Portugal, for financial support under the Ciência 2008 program. D.J.R.D. gratefully acknowledges a grant from the EuroTANGO II Erasmus Mundus Program that made possible his stay at Porto. D.J.R.D. also acknowledges the Universidad Nacional del Nordeste (UNNE) and Consejo Nacional de Investigaciones Científicas y Técnicas of Argentina (CONICET).

REFERENCES

(1) Díaz-Cruz, M. S.; Barceló, D. Chemical Analysis and Ecotoxicological Effects of Organic UV-Absorbing Compounds in Aquatic Ecosystems. *Trends Anal. Chem.* **2009**, *28*, 708−717.

(2) Shaath, N. A. Ultraviolet Filters. *Photochem. Photobiol. Sci.* **2010**, *9*, 464−469.

(3) Hansen, K. V.; Winther, M.; Spanget-Larsen, J. Intramolecular Hydrogen Bonding. Spectroscopic and Theoretical Studies of Vibrational Transitions in Dibenzoylmethane Enol. *J. Mol. Struct.* **2006**, *790*, 74−79.

(4) Tayyari, S. F.; Rahemi, H.; Nekoei, A. R.; Zahedi-Tabrizi, M.; Wang, Y. A. Vibrational Assignment and Structure of Dibenzoylmethane. A Density Functional Theoretical Study. *Spectrochim. Acta Part A* **2007**, *66*, 394−404.

(5) Bertolasi, V.; Ferretti, V.; Gilli, P.; Yao, X.; Li, C.-J. Substituent Effects on Keto-Enol Tautomerization of β-Diketones from X-Ray Structural Data and DFT calculations. *New J. Chem.* **2008**, *32*, 697−704.

(6) Bertolasi, V.; Gilli, P.; Ferretti, V.; Gilli, G. Evidence for Ressonance-Assisted Hydrogen Bonding. 2. Intercorrelation Between Crystal Structure and Spectroscopic Parameters in Eight Intramolecularly Hydrogen Bonded 1,3-Diaryl-1,3-propanedione Enols. *J. Am. Chem. Soc.* **1991**, *113*, 4917−4925.

(7) Gilli, G.; Belluci, F.; Ferretti, V.; Bertolasi, V. Evidence for Ressonance-Assisted Hydrogen Bonding from Crystal-Structure Correlations on the Enol Form of the β-Diketone Fragment. *J. Am. Chem. Soc.* **1989**, *111*, 1023−1028.

(8) Mturi, G. J.; Martincigh, B. S. Photostability of the Sunscreening Agent 4-*tert*-Butyl-4′-methoxydibenzoylmethane (Avobenzone) in Solvents of Different Polarity and Proticity. *J. Photochem. Photobiol., A* **2008**, *200*, 410−420.

(9) Huong, S. P.; Rocher, E.; Fourneron, J.-D.; Charles, L.; Monnier, V.; Bun, H.; Andrieu, V. Photoreactivity of the Sunscreen Butylmethoxydibenzoylmethane (DBM) under Various Experimental Conditions. *J. Photochem. Photobiol., A* **2008**, *196*, 106−112.

(10) Schwack, W.; Rudolph, T. Photochemistry of Dibenzoyl Methane UVA Filters Part 1. *J. Photochem. Photobiol., B* **1995**, *28*, 229−234.

(11) Santos, A. J. M.; Miranda, M. S.; Esteves da Silva, J. C. G. The Degradation Products of UV Filters in Aqueous and Chlorinated Aqueous Solutions. *Water Res.* **2012**, *46*, 3167−3176.

(12) Karlsson, I.; Hillerstrom, L.; Stenfeldt, A.-L.; Martensson, J.; Borje, A. Photodegradation of Dibenzoylmethanes: Potential Cause of Photocontact Allergy to Sunscreens. *Chem. Res. Toxicol.* **2009**, *22*, 1881−1892.

(13) Díaz-Cruz, M. S.; Llorca, M.; Barceló, D. Organic UV filters and their Photodegradates, Metabolites and Disinfection By-products in the Aquatic Environment. *Trends Anal. Chem.* **2008**, *27*, 873−887.

(14) Giokas, D. L.; Salvador, A.; Chisvert, A. UV Filters: From Sunscreens to Human Body and the Environment. *Trends Anal. Chem.* **2007**, *26*, 360−374.

(15) Becke, A. D. Density-Functional Thermochemistry. III. The Role of Exact Exchange. *J. Chem. Phys.* **1993**, *98*, 5648−5652.

(16) Becke, A. D. Density-Functional Exchange-Energy Approximation with Correct Asymptotic Behavior. *Phys. Rev. A* **1988**, *38*, 3098−3100.

(17) Lee, C.; Yang, W.; Parr, R. G. Development of the Colle-Salvetti Correlation-Energy Formula into a Functional of the Electron Density. *Phys. Rev. B* **1988**, *37*, 785−789.

(18) Cossi, M.; Barone, V.; Cammi, R.; Tomasi, J. Ab Initio Study of Solvated Molecules: A New Implementation of the Polarizable Continuum Model. *Chem. Phys. Lett.* **1996**, *255*, 327−335.

(19) Cancès, E.; Mennunci, B.; Tomasi, J. A New Integral Equation Formalism for the Polarizable Continuum Model: Theoretical Background and Applications to Isotropic and Anisotropic Dielectrics. *J. Chem. Phys.* **1997**, *107*, 3032−3041.

(20) Barone, V.; Cossi, M.; Tomasi, J. Geometry Optimization of Molecular Structures in Solution by the Polarizable Continuum Model. *J. Comput. Chem.* **1998**, *19*, 404−417.
(21) Scalmani, G.; Frisch, M. J.; Mennucci, B.; Tomasi, J.; Cammi, R.; Barone, V. Geometries and Properties of Excited States in the Gas Phase and in Solution: Theory and Application of a Time-Dependent Density Functional Theory Polarizable Continuum Model. *J. Chem. Phys.* **2006**, *124*, 094107−15.
(22) Yanai, T.; Tew, D. P.; Handy, N. C. A New Hybrid Exchange-Correlation Functional Using the Coulomb-Attenuating Method (CAM-B3LYP). *Chem. Phys. Lett.* **2004**, *393*, 51−57.
(23) Adamo, C.; Jacquemin, D. The Calculations of Excited-State Properties with Time-Dependent Density Functional Theory. *Chem. Soc. Rev.* **2013**, *42*, 845−856.
(24) Allouche, A. R. Gabedit—A Graphical User Interface for Computational Chemistry Softwares. *J. Comput. Chem.* **2011**, *32*, 174−182.
(25) Frisch, M. J.; Trucks, G. W.; Schlegel, H. B.; Scuseria, G. E.; Robb, M. A.; Cheeseman, J. R.; Scalmani, G.; Barone, V.; Mennucci, B.; Petersson, G. A. et al.*Gaussian 09*, revision A.02; Gaussian, Inc.: Wallingford, CT, 2009.
(26) Bader, R. F. W. Atoms in Molecules. *Acc. Chem. Res.* **1985**, *18*, 9−15.
(27) Lu, T.; Chen, F. Multiwfn: A Multifunctional Wavefunction Analyzer. *J. Comput. Chem.* **2012**, *33*, 580−592.
(28) Shaik, S.; Danovich, D.; Wu, W.; Hiberty, P. C. Charge-Shift Bonding and its Manifestations in Chemistry. *Nature Chem.* **2009**, *1*, 443−449.
(29) Rzepa, H. S. Nature of the Carbon−Sulfur Bond in the Species H−CS−OH. *J. Chem. Theory Comput.* **2011**, *7*, 97−102.
(30) Mitra, S.; Chandra, A. K.; Gashnga, P. M.; Jenkins, S.; Kirk, S. R. Exploring Hydrogen Bond in the Excited State Leading Toward Intramolecular Proton Transfer: Detailed Analysis of the Structure and Charge Density Topology Along the Reaction Path Using QTAIM. *J. Mol. Model.* **2012**, *18*, 4225−4237.
(31) Nasiri, M.; Shakourian-Fard, M.; Fattahi, A. Influence of the Hydrogen Bonding on the Basicity of Selected Macrocyclic Amines. *J. Phys. Org. Chem.* **2012**, *25*, 803−810.
(32) Rozas, I.; Alkorta, I.; Elguero, J. Behavior of Ylides Containing N, O, and C Atoms as Hydrogen Bond Accepters. *J. Am. Chem. Soc.* **2000**, *122*, 11154−11161.
(33) Pinto da Silva, L.; Simkovitch, R.; Huppert, D.; Esteves da Silva, J. C. G. Theoretical Study of the Efficient Fluorescence Quenching Process of the Firefly Luciferin. *J. Photochem. Photobiol,. A* **2013**, *266*, 47−54.
(34) Paul, B. K.; Mahanta, S.; Singh, R. B.; Guchhait, N. A DFT-based Theoretical Study on the Photophysics of 4-Hydroxyacridine: Single-water-mediated Excited State Proton Transfer. *J. Phys. Chem. A* **2010**, *114*, 2618−2627.
(35) Mahanta, S.; Paul, B. K.; Singh, R. B.; Guchchait, N. Inequivalence of Substitution Pairs in Hydroxynaphthaldehyde: A Theoretical Measurement by Intramolecular Hydrogen Bond Strength, Aromaticity, and Excited-state Intramolecular Proton Transfer Reaction. *J. Comput. Chem.* **2011**, *32*, 1−14.